A novel role for activating transcription factor-2 in 15(S)-hydroxyeicosatetraenoic acid-induced angiogenesis

Tieqiang Zhao,[2,*] Dong Wang,[2,*] Sergey Y. Cheranov,[*] Manjula Karpurapu,[*] Koteswara R. Chava,[*] Venkatesh Kundumani-Sridharan,[*] Dianna A. Johnson,[†] John S. Penn,[§] and Gadiparthi N. Rao[1,*]

Department of Physiology,* University of Tennessee Health Science Center, Memphis, TN 38163; Department of Ophthalmology,† University of Tennessee Health Science Center, Memphis, TN 38163; and Vanderbilt Eye Institute,§ Vanderbilt University School of Medicine, Nashville, TN 37232

Abstract To investigate the mechanisms underlying 15(S)-HETE-induced angiogenesis, we have studied the role of the small GTPase, Rac1. We find that 15(S)-HETE activated Rac1 in human retinal microvascular endothelial cells (HRMVEC) in a time-dependent manner. Blockade of Rac1 by adenovirus-mediated expression of its dominant negative mutant suppressed HRMVEC migration as well as tube formation and Matrigel plug angiogenesis. 15(S)-HETE stimulated Src in HRMVEC in a time-dependent manner and blockade of its activation inhibited 15(S)-HETE-induced Rac1 stimulation in HRMVEC and the migration and tube formation of these cells as well as Matrigel plug angiogenesis. 15(S)-HETE stimulated JNK1 in Src-Rac1-dependent manner in HRMVEC and adenovirus-mediated expression of its dominant negative mutant suppressed the migration and tube formation of these cells and Matrigel plug angiogenesis. 15(S)-HETE activated ATF-2 in HRMVEC in Src-Rac1-JNK1-dependent manner and interference with its activation via adenovirus-mediated expression of its dominant negative mutant abrogated migration and tube formation of HRMVEC and Matrigel plug angiogenesis. In addition, 15(S)-HETE-induced MEK1 stimulation was found to be dependent on Src-Rac1 activation. Blockade of MEK1 activation inhibited 15(S)-HETE-induced JNK1 activity and ATF-2 phosphorylation. Together, these findings show that 15(S)-HETE activates ATF-2 via the Src-Rac1-MEK1-JNK1 signaling axis in HRMVEC leading to their angiogenic differentiation.—Zhao, T., D. Wang, S. Y. Cheranov, M. Karpurapu, K. R. Chava, V. Kundumani-Sridharan, D. A. Johnson, J. S. Penn, and G. N. Rao. **A novel role for activating transcription factor-2 in 15(S)-hydroxyeicosatetraenoic acid-induced angiogenesis. *J. Lipid Res.* 2009.** 50: **521–533.**

Supplementary key words eicosanoid • Rac1 • retinal neovascularization

Two 15-lipoxygenases (15-LOXs), namely, 15-LOX1 and 15-LOX2, have been shown to be present in humans (1, 2). Both enzymes metabolize linoleic acid (LA) to 13(S)-hydroperoxyoctadecadienoic acid [13(S)-HPODE] and arachidonic acid (AA) to 15(S)-hydroperoxyeicosatetraenoic acid [15(S)-HPETE] preferentially (3, 4). With regard to their tissue distribution, while 15-LOX1 shows a narrow cell-specific expression, including human reticulocytes and airway epithelial cells, 15-LOX2 appears to be expressed in epithelial cell types in cornea, lung, prostate, and skin (5). Although the presence of 15-LOX2 in the vessel wall has yet to be reported, vascular smooth muscle cells (VSMC) and endothelial cells (EC) express 15-LOX1 (also known as 12/15-LOX in murines) and when exposed to AA, these cells produce 15(S)-HETE and 12(S)-HETE (6–9). A number of studies have demonstrated that 15-LOX1 and its murine ortholog 12/15-LOX play a role in atherosclerosis (10–12). In addition, human atheroma homogenates upon incubation converted AA mainly to 15-HETE (13). A possible role for 15-LOX1 and 15-LOX2 in carcinomas is suggested by studies showing that the expression levels of 15-LOX1 and 12/15-LOX correlate with tumor grade in human and murine prostate cancers (14, 15). On the other hand, the expression levels of 15-LOX2 were decreased in prostate carcinomas (16, 17). Although 15-LOX1 and 12/15-LOX convert AA to 15(S)-HETE and 12(S)-HETE, respectively, only the latter eicosanoid mimicked these enzymes in stimulating prostate cancer cell proliferation (18, 19). 15(S)-HETE although is the major product of AA produced by 15-LOX1 and 15-LOX2; however, it mimics the actions of only 15-LOX2 but not 15-LOX1, at least in the regulation of prostate tumor growth (20–22). In fact, many studies reported that 15(S)-HETE induces apoptosis in various cancer cell types (21, 22).

In contrast to the above-mentioned observations, some reports provided clues that 15(S)-HETE induces retinal angiogenesis (23, 24). Angiogenesis plays a critical role in the progression of various diseases including atherosclero-

This work was supported by a grant (EY014856) from the National Eye Institute/National Institutes of Health.

Manuscript received 23 July 2008 and in revised form 1 October 2008 and in re-revised form 7 October 2008.

Published, JLR Papers in Press, October 10, 2008
DOI 10.1194/jlr.M800388-JLR200

[1] To whom correspondence should be addressed.
e-mail: grao@physio1.utmem.edu
[2] T. Zhao and D. Wang contributed equally to this work.

sis, tumors, and diabetic retinopathy (25–27). To learn more about the capacity of 15(S)-HETE in the stimulation of angiogenesis, we reported that it induces the migration and tube formation of microvascular endothelial cells from different vascular beds (8, 28, 29). Substantial evidence shows that Rac1, a small GTPase protein, plays a major role in the regulation of cell motility (30–32). We have previously shown that 15(S)-HETE-induced angiogenesis requires activation of ERK1/2 and JNK1 (8). Rac1 plays a role in the activation of JNK1 (33). Toward understanding the mechanisms of 15(S)-HETE-induced angiogenesis, here we report that 15(S)-HETE-induced JNK1 activation requires Src-dependent Rac1-mediated MEK1 stimulation and that Src-Rac1-MEK1-JNK1 signaling targets ATF-2 in influencing human retinal microvascular endothelial cell (HRMVEC) angiogenic differentiation.

MATERIALS AND METHODS

Reagents

Arachidonic acid and 15(S)-HETE were bought from Cayman Chemicals (Ann Arbor, MI). Growth factor-reduced Matrigel (Cat. No. 354250) was obtained from BD Biosciences (Bedford, MA). Phosphospecific anti-Src (Tyr416) (Cat. No. 2101), phosphospecific anti-MEK1/2 (Ser217/221) (Cat. No. 9121), phosphospecific anti-SAPK/JNK (Thr183/Tyr185) (Cat. No. 9251), and phosphospecific anti-ATF-2 (Thr69/71) (Cat. No. 9225) antibodies were obtained from Cell Signaling Technology (Beverly, MA). Anti-Rac1 (Cat. No. 05-389) and anti-Src antibodies (Cat. No. 05-184) were obtained from Upstate Biotechnology Inc. (Lake Placid, NY). Anti-MEK1 (Cat. No. SC-219), and anti-JNK1 (Cat. No. SC-474) and anti-ATF-2 (Cat. No. SC-187) antibodies were purchased from Santa Cruz Biotechnology Inc. (Santa Cruz, CA). Anti-CD31 antibodies (Cat. No. 550274) were purchased from BD Pharmingen (Palo Alto, CA). T4 polynucleotide kinase was procured from New England Biolabs (Ipswich, MA). [γ ^{32}P] ATP (3,000 Ci/mmol) was bought from GE Healthcare Biosciences (Piscataway, NJ). All experiments involved the use of animals were approved by the Animal Care and Use Committee of the University of Tennessee Health Science Center, Memphis, TN.

Adenoviral vectors

The construction of pAd-GFP and pAd-dnMEK1 were described previously (34). To clone dnRac1 into adenoviral vector, Rac1N17 was released from pCEV-Rac1N17 by digestion with BamHI and *Eco*RI (35) and subcloned into the same sites of pENTR3C to yield pENTR3C-Rac1N17. The pENTR3C-Rac1N17 was then subjected to recombination with pAdCMVV5DEST to obtain pAd-Rac1N17. To construct adenoviral vector for dnJNK1, Flag-JNK1apf was released from pCDNA1FlagJNK1apf by digestion with *Hind*III and XbaI (36) and subcloned into the same sites of pBluescript II SK (+). The Flag-JNK1apf was excised by digestion with KpnI and NotI and cloned into the same sites of pENTR3C to yield pENTR3C-flag-JNK1apf. The pENTR3C-flag-JNK1apf was recombinated with pAdCMVV5DEST to yield pAd-flag-JNK1apf. To make adenoviral vector for dnATF-2, dnATF-2 fragment was released from pCDNA3-dnATF-2 by digestion with KpnI and NotI (37) and cloned into the same sites of pENTR3C to yield pENTR3C-dnATF-2, which was then recombinated with pAdCMVV5DEST to yield pAd-dnATF-2. The plasmids, pAd-GFP, pAd-dnMEK1, pAd-Rac1N17 pAd-dnATF-2, and pAd-flag-JNK1apf were linearized by digestion with PacI and transfected into HEK293A cells. The resultant adenovirus was further amplified by infection of HEK293A cells and was purified by cesium chloride gradient ultracentrifugation (38). The construction of Ad-dnSrc was described previously (39) and provided by Dr. Richard C. Vanema of Georgia Medical College, Augusta, GA.

Cell culture

Primary HRMVEC (Cat. No. ACBRI 181) were bought from Applied Cell Biology Research Institute (Kirkland, WA). Cells were grown in medium 131 containing microvascular growth supplements, 10 μg/ml gentamycin, and 0.25 μg/ml amphotericin B. Cultures were maintained at 37°C in a humidified 95% air and 5% CO_2 atmosphere. Cells were quiesced by incubating in medium 131 for 24 h and used between 4 to 10 passages to perform the experiments unless otherwise indicated. 15(S)-HETE was added to cells in ethanol. Thus, controls received an equal volume of ethanol and it does not exceed 0.03%.

Pull-down assay

To measure Rac1 activation, an equal amount of protein from control and each treatment was incubated with GST-PAK1 beads overnight at 4°C. After collection by centrifugation, the beads were heated in 50 μl of Laemmeli sample buffer for 10 min, and the released proteins were resolved by 0.1% SDS-12% PAGE followed by Western blot analysis for Rac1 using its specific antibodies.

JNK1 assay

JNK1 activity was measured by immunocomplex kinase assay as described previously (40). Protein extracts from cells or tissues were prepared using lysis buffer (20 mM HEPES, pH 7.4, 150 mM NaCl, 1% NP-40, 10 μg/ml aprotinin, 10 μg/ml leupeptin, 50 mM glycerophosphate, 10 mM NaF, and 1 mM sodium orthovanadate). Equal amount of protein (200 μg) from each sample was immunoprecipitated with anti-JNK1/2 antibodies (2 μg) overnight at 4°C followed by incubation with protein-A sepharose beads for 1 h at room temperature. The immunocomplexes were washed four times with lysis buffer, one time with kinase buffer, and incubated in kinase reaction mix containing 25 mM HEPES (pH 7.4), 10 mM $MgCl_2$, 1 mM EGTA, 200 μg/ml GST-c-Jun fusion protein, 1 μCi [γ^{32}P]ATP, and 50 μM ATP for 30 min at 30°C. The kinase reactions were stopped by addition of SDS-PAGE sample buffer and subsequent boiling for 5 min. The reaction products were separated by electrophoresis on 0.1% SDS and 10% polyacrylamide gels. The [^{32}P]labeled GST-c-Jun protein was visualized by autoradiography and the band intensities were quantified using NIH Image J.

Cell migration assay

Cell migration was performed using a modified Boyden Chamber method as described by Nagata, Mogi, and Walsh (41). The cell culture inserts containing membranes with 10 mm in diameter and 8.0 μm pore size (Nalge Nunc International, Rochester, NY) were placed in a 24-well tissue culture plate (Costar, Corning Incorporated, Corning, NY). The lower surface of the porous membrane was coated with 70% Matrigel at 4°C overnight and then blocked with 0.1% heat-inactivated BSA at 37°C for 1 h. HRMVEC were quiesced for 24 h in medium 131, trypsinized, and neutralized with trypsin neutralizing solution. Cells were seeded into the upper chamber at 1×10^5 cells/well. Vehicle or 15(S)-HETE were added to the lower chamber at the indicated concentration. The upper and lower chambers contained medium 131. When the effect of dominant negative Src, Rac1, JNK1, and ATF-2 mutants was tested on 15(S)-HETE-induced HRMVEC migration, cells were infected with Ad-GFP, Ad-dnSrc,

Ad-dnRac1, Ad-dnJNK1, or Ad-dnATF-2 at a moi of 80 and quiesced before they were subjected to the migration assay. After 6 h of incubation at 37°C, nonmigrated cells were removed from the upper side of the membrane with cotton swabs and the cells on the lower surface of the membrane were fixed in methanol for 15 min. The membrane was then stained with Hematoxylin and observed under a light microscope (Eclipse 50i, Nikon, Japan). Images were captured using a Nikon Digital Sight DS-L1 system. Cells were counted in five randomly selected squares per well and presented as the number of migrated cells/field.

Tube formation assay

Tube formation assay was performed as described by Nagata, Mogi, and Walsh (41). Twenty-four well culture plates (Costar, Corning Incorporated) were coated with growth factor-reduced

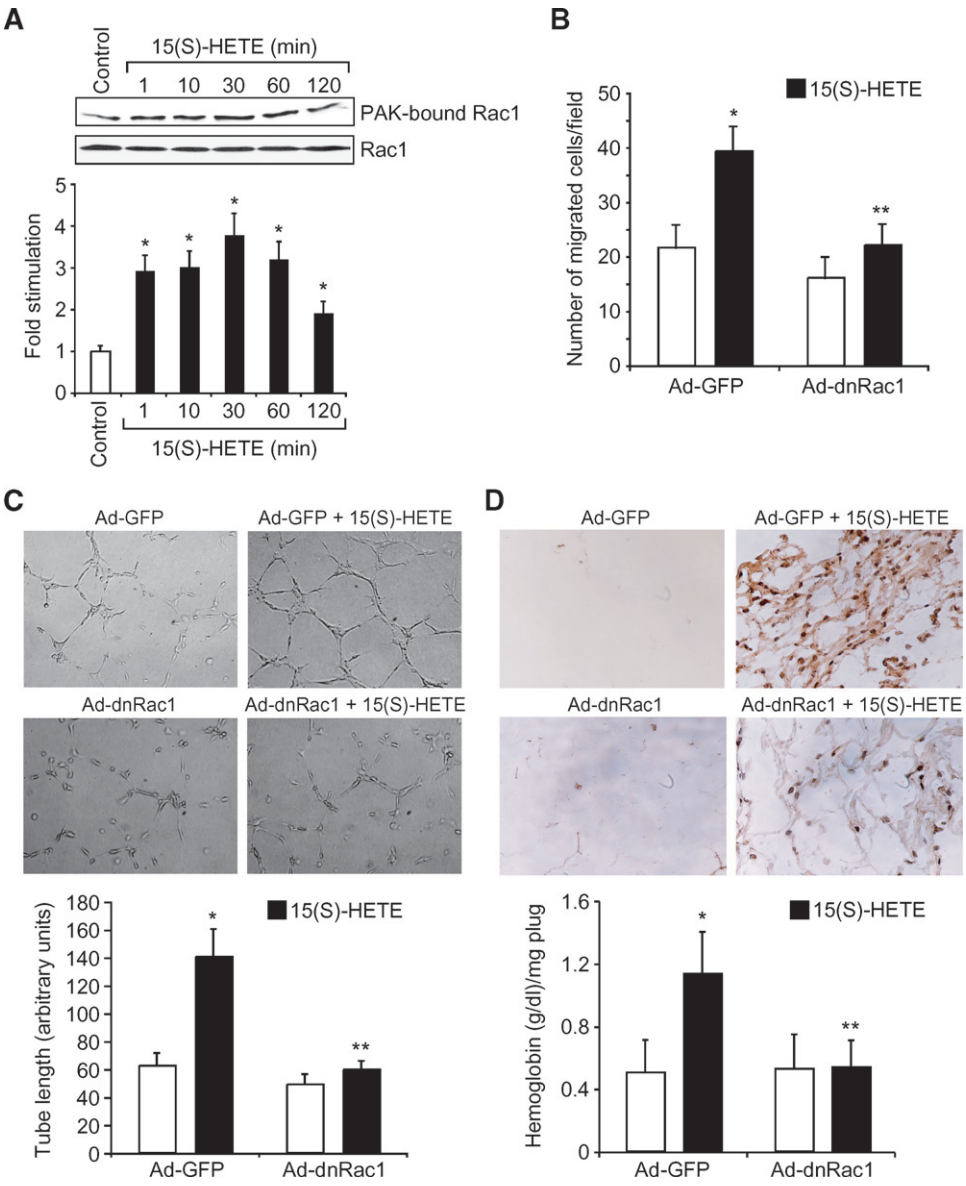

Fig. 1. 15(S)-HETE-induced angiogenic differentiation of human retinal microvascular endothelial cells (HRMVEC) requires Rac1 activation. A: Quiescent HRMVEC were treated with and without 15(S)-HETE (0.1 μM) for the indicated times and cell extracts were prepared and analyzed for Rac1 activation by pull-down assay. Cellular total Rac1 levels are shown in the lower panel. B, C: HRMVEC were transduced with Ad-GFP or Ad-dnRac1 at a moi of 80, quiesced, and subjected to 15(S)-HETE-induced migration (B) or tube formation (C). D: C57BL/6 mice were injected subcutaneously with 0.5 ml of Matrigel premixed with vehicle or 50 μM 15(S)-HETE with and without Ad-GFP or Ad-dnRac1 (5×10^9 pfu/ml). One week later, the animals were sacrificed, and the Matrigel plugs were harvested from underneath the skin and either immunostained for CD31 expression using anti-CD31 antibodies or analyzed for hemoglobin content using Drabkin's reagent. The values in the bar graphs in panels A, B, C, and D are the means ± SD of three independent experiments or four plugs from four animals. * $P < 0.01$ vs. control or Ad-GFP; ** $P < 0.01$ vs. Ad-GFP + 15(S)-HETE. The white bars represent controls to their respective treatments.

Matrigel (BD Biosciences) in a total volume of 280 μl/well and allowed to solidify for 30 min at 37°C. HRMVEC were trypsinized, neutralized with trypsin neutralizing solution, and resuspended in medium 131 at 5×10^5/ml and 200 μl of this cell suspension was added into each well. Vehicle or 15(S)-HETE, at the indicated concentration, were added to the appropriate well and the cells were incubated at 37°C for 6 h. When the effect of dominant negative Src, Rac1, JNK1, and ATF-2 mutants was tested on 15(S)-HETE-induced HRMVEC tube formation, cells were infected with Ad-GFP, Ad-dnSrc, Ad-dnRac1, Ad-dnJNK1 or Ad-dnATF-2 at a moi of 80 and quiesced before they were subjected to tube formation. Tube formation was observed under an inverted microscope (Model, Eclipse TS100, Nikon, Japan). Images were captured with a CCD color camera (Model, KP-D20AU, Hitachi, Japan) attached to the microscope and tube length was measured using the NIH Image J.

Western blot analysis

After appropriate treatments and rinsing with cold PBS, HRMVEC were lysed in 500 μl of lysis buffer (PBS, 1% Nonidet P-40, 0.5% sodium deoxycholate, 0.1% SDS, 100 μg/ml PMSF, 100 μg/ml aprotinin, 1 μg/ml leupeptin and 1 mM sodium orthovanadate) and scraped into 1.5 ml Eppendorf tubes. After standing on ice for 20 min, the cell lysates were cleared by centrifugation at 12,000 rpm for 20 min at 4°C. Samples of cell lysates containing an equal amount of protein were resolved by electrophoresis on 0.1% SDS and 10% polyacrylamide gels. The proteins were transferred electrophoretically to a nitrocellulose membrane (Hybond, Amersham Pharmacia Biotech, Piscataway, NJ). After blocking in 10 mM Tris-HCl buffer, pH 8.0, containing 150 mM sodium chloride, 0.1% Tween 20 and 5% (w/v) nonfat dry milk, the membrane was treated with appropriate primary antibodies followed by incubation with Horseradish Peroxidase (HRP)-conjugated secondary antibodies. The antigen-antibody complexes were detected using chemiluminescence reageant kit (Amersham Pharmacia Biotech, Piscataway, NJ).

Matrigel plug angiogenesis assay

Matrigel plug assay was performed essentially as described by Medhora et al. (42). C57BL/6 mice (8 wks old) were lightly anesthetized with sodium pentobarbital (50 mg/kg, i.p.) and were injected subcutaneously with 0.5 ml of Matrigel that was premixed with vehicle or 50 μM of 15(S)-HETE along the dorsal midline. Although this high concentration of 15(S)-HETE was used in the Matrigel plug angiogenesis experiments during the course of the present study, ongoing experiments showed that 15(S)-HETE even at much lower concentrations (5 μM) also induces Matrigel plug angiogenesis to a level similar to that of 50 μM. The injection was made rapidly with a B-D 26G1/2 needle to ensure the entire content was delivered as a single plug. Whenever the effects of Ad-GFP, Ad-dnSrc, Ad-dnRac1, Ad-dnJNK1, or Ad-dnATF-2 (5×10^9 pfu/ml) were tested on 15(S)-HETE-induced angiogenesis, these adenoviruses were added to the Matrigel prior to the injection. The mice were allowed to recover and 7 days later, unless otherwise stated, the animals were sacrificed by inhalation of CO_2 and the Matrigel plugs were harvested from underneath the skin. The plugs were homogenized in 1 ml of deionized H_2O on ice and cleared by centrifugation at 10,000 rpm for 6 min at 4°C. The supernatant was collected and used to measurements of hemoglobin content with Drabkin's reagent along with hemoglobin standard essentially according to the manufacturer's protocol (Sigma Chemical Co.). The absorbance was read at 540 nm in an ELISA plate reader (Spectra Max 190, Molecular Devices, Sunnyvale, CA). These experiments were repeated at least three times with four mice for each group, and the values are expressed as g/dl of hemoglobin/mg plug.

Immunohistochemistry

After retrieving the Matrigel plugs from mice, they were snap-frozen in OCT compound. Cryo-sections (5 μm) were made using Leica Cryostat machine (Model: CM3050S) and stained with anti-CD31 antibody (1:500 dilution, BD Pharmingen, Palo Alto, CA), followed by sequential incubation with biotinylated

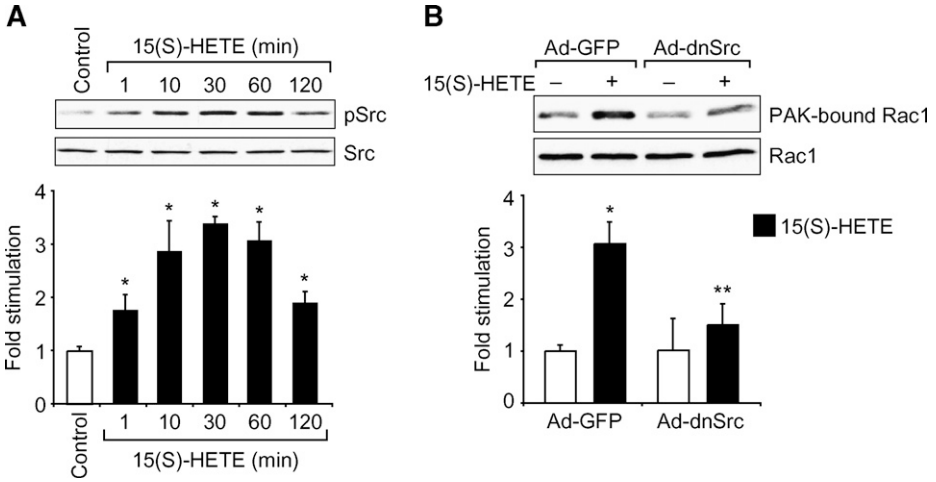

Fig. 2. Src mediates 15(S)-HETE-induced Rac1 activation in HRMVEC. A: Quiescent HRMVEC were treated with and without 15(S)-HETE (0.1 μM) for the indicated times and cell extracts were prepared and analyzed for Src activation by Western blotting using its phospho-specific antibodies. For normalization, the same blot was reprobed with anti-Src antibodies. B: HRMVEC were transduced with Ad-GFP or Ad-dnSrc at a moi of 80, quiesced, treated with and without 15(S)-HETE (0.1 μM) for 10 min, and cell extracts were prepared and analyzed for Rac1 activation by pull-down assay. The values in the bar graphs in panels A and B are the means ± SD of three independent experiments. * $P < 0.01$ vs. control or Ad-GFP; ** $P < 0.01$ vs. Ad-GFP + 15(S)-HETE. The white bars represent controls to their respective treatments.

anti-rat IgG (1:300 dilution), avidin-biotin peroxidase, and diaminobenzidine substrate (Vector Laboratories, Burlingame, CA). The sections were counterstained with Hematoxylin and examined under a light microscope (Model: Eclipse 50i, Nikon, Japan) in six random fields (400× magnification) from each group. Images were captured using Nikon Digital Sight DS-L1 system.

Statistics

All the experiments were repeated three times and data are presented as Means ± SD. The treatment effects were analyzed by Student's *t*-test and the *P* values < 0.05 were considered to be statistically significant. In the case of Western blotting, one representative set of data is shown.

RESULTS

15(S)-HETE activates Rac1 in HRMVEC

Previously we have demonstrated that 15(S)-HETE induces HRMVEC migration more potently than 5(S)-HETE or 12(S)-HETE. In addition, we reported that 15(S)-HETE induces angiogenic differentiation of HRMVEC involving MEK1-dependent activation of ERK1/2 and JNK1 (8). To investigate further the mechanisms by which 15(S)-HETE induces retinal angiogenesis, here we have studied the role of Rac1. Quiescent HRMVEC were treated with and without 15(S)-HETE (0.1 μM) for the indicated times and an equal amount of protein from control each treat-

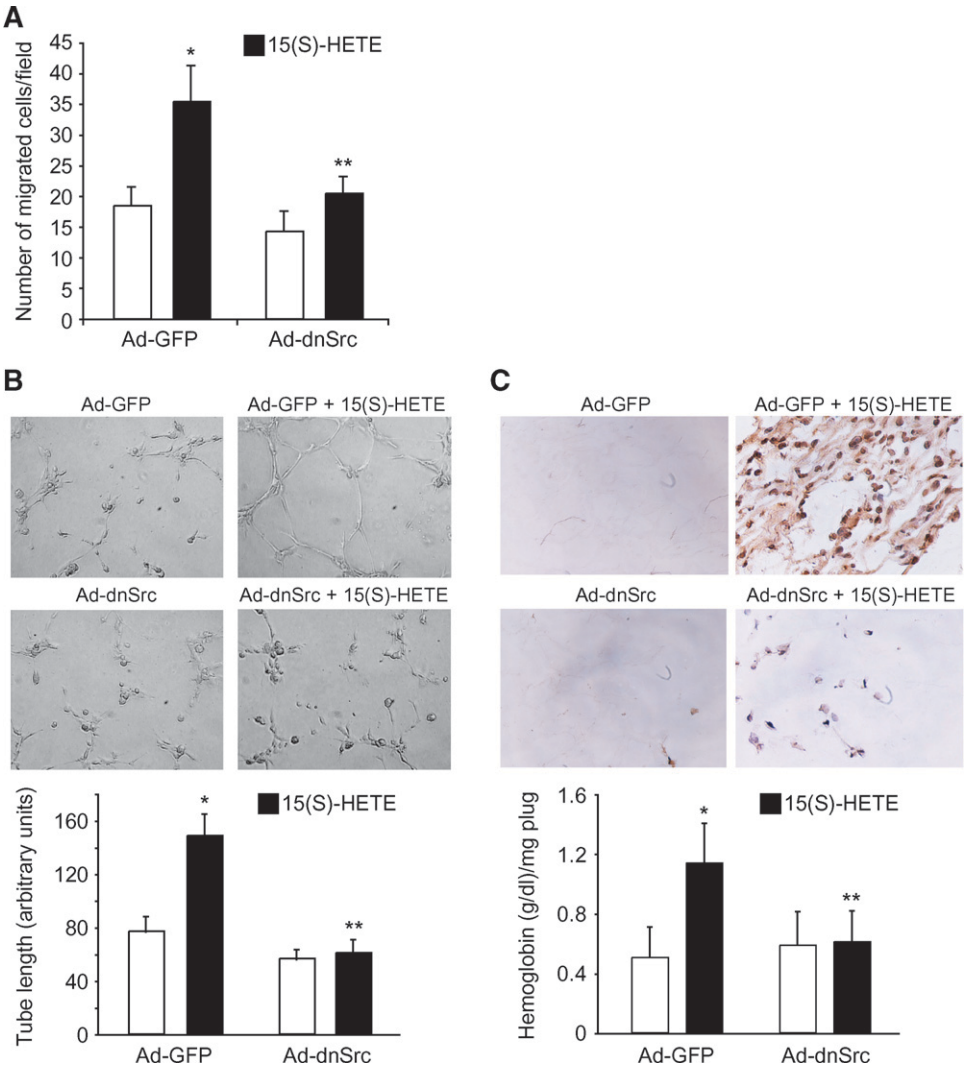

Fig. 3. Blockade of Src activation suppresses 15(S)-HETE-induced HRMVEC migration and tube formation in vitro and Matrigel plug angiogenesis in vivo. A, B: HRMVEC were transduced with Ad-GFP or Ad-dnSrc at a moi of 80, quiesced, and subjected to 15(S)-HETE-induced migration (A) or tube formation (B). C: C57BL/6 mice were injected subcutaneously with 0.5 ml of Matrigel premixed with vehicle or 50 μM 15(S)-HETE with and without Ad-GFP or Ad-dnSrc (5×10^9 pfu/ml). One week later, the animals were sacrificed, and the Matrigel plugs were harvested from underneath the skin and either immunostained for CD31 expression using anti-CD31 antibodies or analyzed for hemoglobin content using Drabkin's reagent. The values in the bar graphs in panels A, B, and C are the means ± SD of three independent experiments or four plugs from four animals. * $P < 0.01$ vs. Ad-GFP; ** $P < 0.01$ vs. Ad-GFP + 15(S)-HETE. The white bars represent controls to their respective treatments.

ment was analyzed by pull-down assay for PAK-bound Rac1 as previously described. 15(S)-HETE stimulated Rac1 activation in a time-dependent manner with a near maximum 3-fold increase at 10 min that was sustained until 60 min and declined thereafter (**Fig. 1A**). Next we tested the role of Rac1 in 15(S)-HETE-induced HRMVEC migration and tube formation. 15(S)-HETE stimulated HRMVEC migration by approximately 2-fold as measured by a modified Boyden chamber method, and adenovirus-mediated expression of dnRac1 attenuated this effect (Fig. 1B). Similarly, 15(S)-HETE induced HRMVEC tube formation by approximately 2-fold, and this effect was blocked by adenovirus-mediated expression of the dominant negative Rac1 mutant (Fig. 1C). In order to obtain additional evidence for the role of Rac1 in 15(S)-HETE-induced angiogenesis, we used the Matrigel plug angiogenesis model. As shown in Fig. 1D, 15(S)-HETE (50 μM) induced Matrigel plug angiogenesis and dnRac1 significantly inhibited this effect.

Src mediates 15(S)-HETE-induced Rac1 activation in HRMVEC

Many studies have shown that Src mediates Rac1 in response to receptor tyrosine kinase agonists and cytokines (43, 44). To determine whether Src mediates 15(S)-HETE-induced activation of Rac1, we first studied the time course of the effect of this eicosanoid on tyrosine phosphorylation

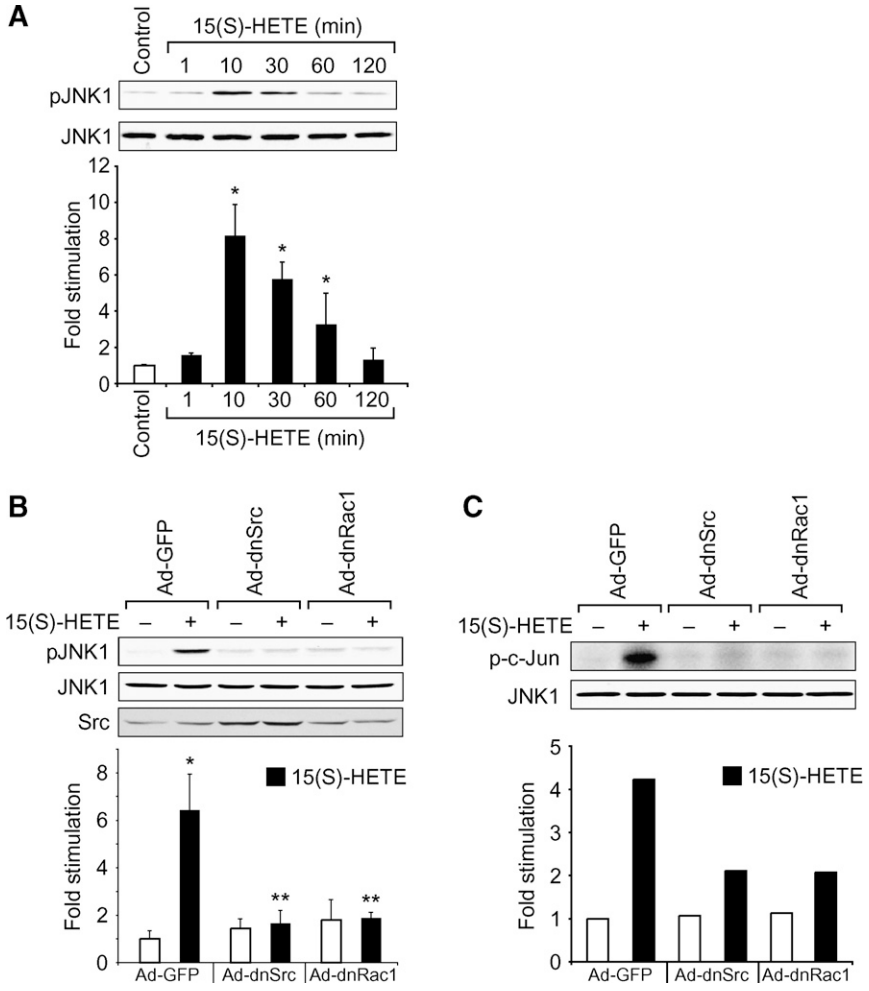

Fig. 4. Src-Rac1 signaling mediates 15(S)-HETE-induced JNK1 activation in HRMVEC. A: Quiescent HRMVEC were treated with and without 15(S)-HETE (0.1 μM) for the indicated times, and cell extracts were prepared and analyzed by Western blotting for pJNK1 using its phosphospecific antibodies. The blot was reprobed with anti-JNK1 antibodies for normalization. B, C: HRMVEC were transduced with Ad-GFP, Ad-dnSrc, or Ad-dnRac1 at a moi of 80, quiesced, treated with and without 15(S)-HETE (0.1 μM) for 10 min, and cell extracts were prepared and analyzed for JNK1 activation either by Western blotting using its phosphospecific antibodies or by immunocomplex kinase assay using GST-c-Jun protein and [γ-^{32}P]ATP as substrates. The blots in panels A and B were reprobed either with anti-JNK1 antibodies for normalization or anti-Src antibodies to show overexpression of Src. The values in the bar graphs in panels A and B are the means ± SD of three independent experiments. * $P < 0.01$ vs. control or Ad-GFP; ** $P < 0.01$ vs. Ad-GFP + 15(S)-HETE. The white bars represent controls to their respective treatments.

of Src. 15(S)-HETE induced the tyrosine (Tyr416) phosphorylation of Src in a time-dependent manner with a maximum 3-fold increase at 10 min, that was sustained for 60 min and declined thereafter (**Fig. 2A**). Next, we tested the effect of dnSrc on 15(S)-HETE-induced activation of Rac1. Adenovirus-mediated expression of dnSrc without affecting the Rac1 levels significantly inhibited its PAK-bound levels (Fig. 2B). To test the role of Src in 15(S)-HETE-induced angiogenic events, we further tested the effect of dnSrc on HRMVEC migration and tube formation and Matrigel plug angiogenesis. Adenovirus-mediated expression of dnSrc completely inhibited 15(S)-HETE-induced HRMVEC migration and tube formation and Matrigel plug angiogenesis (**Fig. 3A–C**).

15(S)-HETE activates JNK1 in HRMVEC via Src-Rac1 signaling

Previously we have shown that 15(S)-HETE stimulates JNK1 in HRMVEC (7). To understand the mechanisms of JNK1 activation by 15(S)-HETE, here we have examined the role of Src and Rac1. 15(S)-HETE activated JNK1 in a time-dependent manner (**Fig. 4A**). Adenovirus-mediated expression of either dnSrc or dnRac1 blocked 15(S)-HETE-induced JNK1 phosphorylation and activity (Fig. 4B, C).

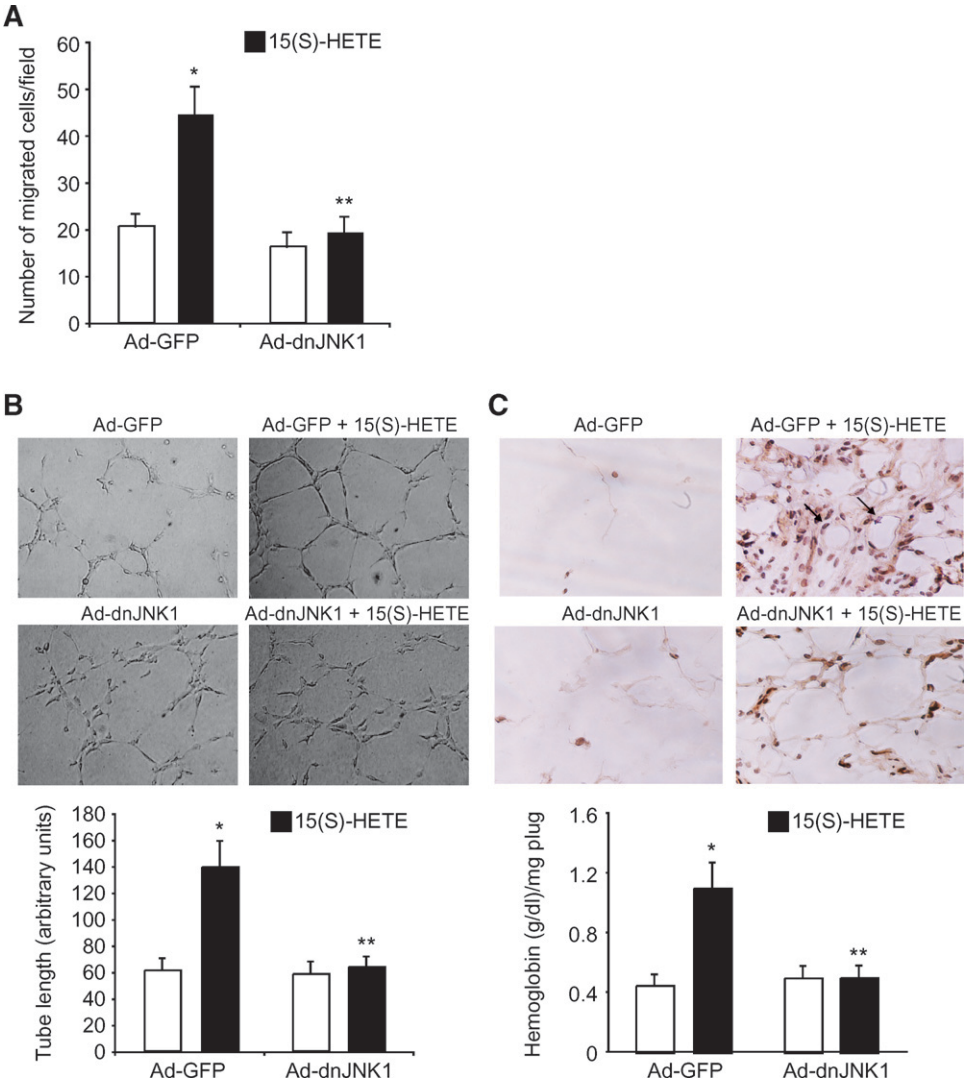

Fig. 5. Adenovirus-mediated expression of dnJNK1 inhibits 15(S)-HETE-induced HRMVEC migration and tube formation in vitro and Matrigel plug angiogenesis in vivo. A, B: HRMVEC were transduced with Ad-GFP or Ad-dnJNK1 at a moi of 80, quiesced, and subjected to 15(S)-HETE-induced migration (A) or tube formation (B). C: C57BL/6 mice were injected subcutaneously with 0.5 ml of Matrigel premixed with vehicle or 50 μM 15(S)-HETE with and without Ad-GFP or Ad-dnJNK1 (5×10^9 pfu/ml). One week later, the animals were sacrificed, and the Matrigel plugs were harvested from underneath the skin and either immunostained for CD31 expression using anti-CD31 antibodies or analyzed for hemoglobin content using Drabkin's reagent. The values in the bar graphs in panels A, B, and C are the means ± SD of three independent experiments or four plugs from four animals. * $P < 0.01$ vs. Ad-GFP; ** $P < 0.01$ vs. Ad-GFP + 15(S)-HETE. The white bars represent controls to their respective treatments.

Blockade of JNK1 activation by adenovirus-mediated expression of its dominant negative mutant significantly blunted 15(S)-HETE-induced HRMVEC migration and tube formation and Matrigel plug angiogenesis (**Fig. 5A**–C).

15(S)-HETE activates ATF-2 in HRMVEC

One of the transcriptional factors shown to be activated by the MAP kinases, particularly, JNKs and p38MAPK, is activating transcription factor-2 (ATF-2) (45–47). Because 15(S)-HETE activated JNK1, we asked whether 15(S)-HETE stimulates ATF-2. 15(S)-HETE activated ATF-2 in a time-dependent manner as measured by its phosphorylation (**Fig. 6A**). To identify the mechanisms of ATF-2 activation, we next studied the role of Src, Rac1, and JNK1. Adenovirus-mediated expression of dnSrc, dnRac1, or dnJNK1 blocked 15(S)-HETE-induced ATF-2 phosphorylation (Fig. 6B, C). Blockade of ATF-2 by adenovirus-mediated expression of its dominant negative mutant significantly blunted 15(S)-HETE-induced migration and tube formation of HRMVEC and Matrigel plug angiogenesis in vivo (**Fig. 7A–C**).

MEK1 mediates 15(S)-HETE-induced ATF-2 via JNK1-dependent manner

Previously we have reported that MEK1 acts as an upstream kinase in 15(S)-HETE-induced JNK1 activation (8). To understand the upstream signaling events of MEK1 activation by 15(S)-HETE in HRMVEC, we studied the role of Src and Rac1. Interference with Src-Rac1 signaling via adenovirus-mediated expression of their dominant negative

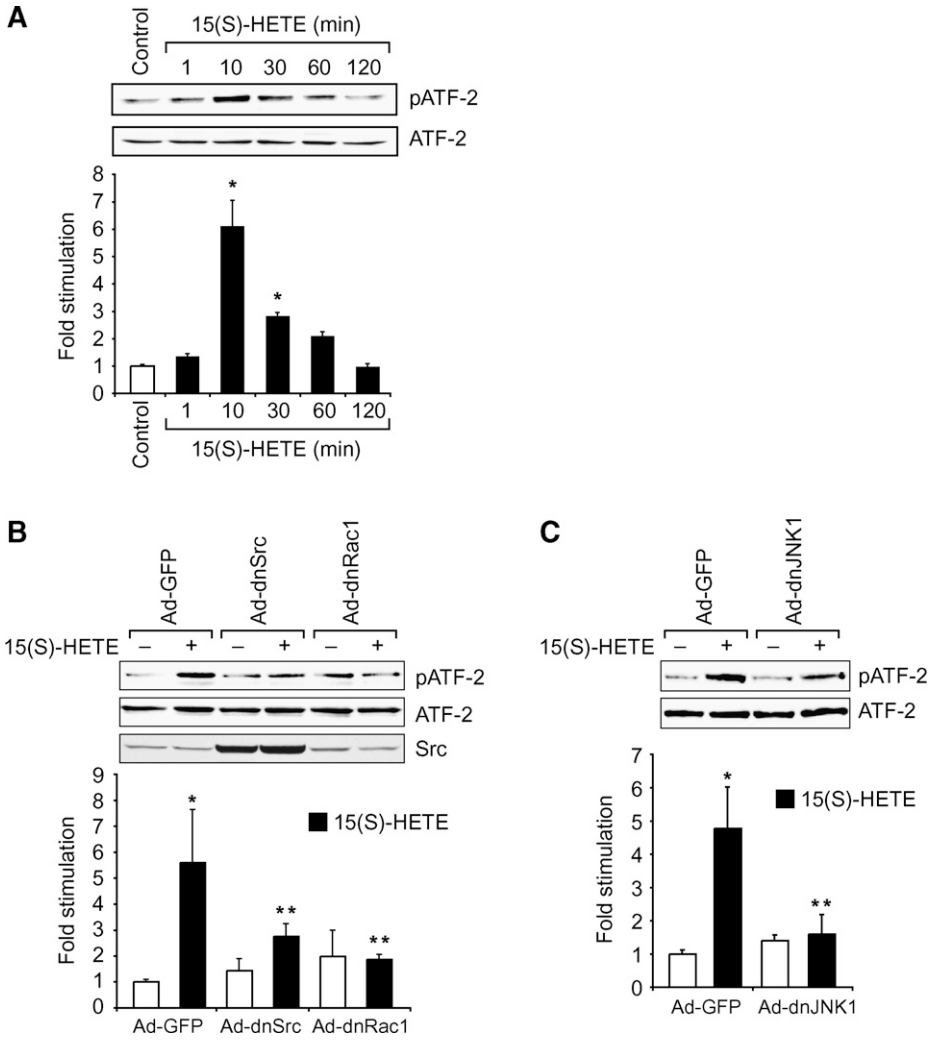

Fig. 6. Src-Rac1-JNK1 signaling mediates 15(S)-HETE-induced ATF-2 activation in HRMVEC. A: Quiescent HRMVEC were treated with and without 15(S)-HETE (0.1 μM) for the indicated times, and cell extracts were prepared and analyzed by Western blotting for pATF-2 using its phosphospecific antibodies. B, C: HRMVEC were transduced with Ad-GFP, Ad-dnSrc, Ad-dnRac1, or Ad-dnJNK1 at a moi of 80, quiesced, treated with and without 15(S)-HETE (0.1 μM) for 10 min, and cell extracts were prepared and analyzed for ATF-2 phosphorylation as described in panel A. The blots in panels A, B, and C were reprobed either with anti-ATF-2 antibodies for normalization or anti-Src antibodies to show overexpression of Src. The values in the bar graphs are the means ± SD of three independent experiments. * $P < 0.01$ vs. control or Ad-GFP; ** $P < 0.01$ vs. Ad-GFP + 15(S)-HETE. The white bars represent controls to their respective treatments.

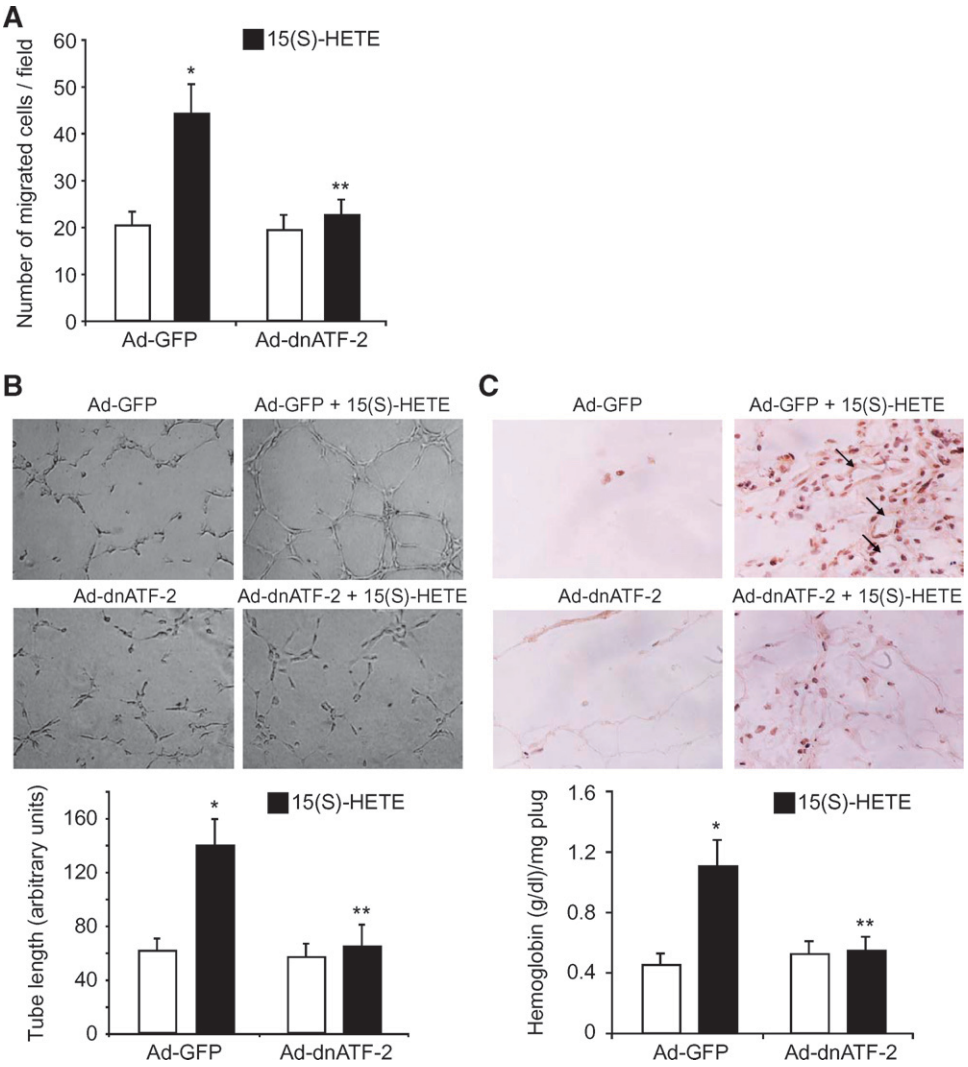

Fig. 7. Adenovirus-mediated expression of dnATF-2 suppresses 15(S)-HETE-induced HRMVEC migration and tube formation in vitro and Matrigel plug angiogenesis in vivo. A, B: HRMVEC were transduced with Ad-GFP or Ad-dnATF-2 at a moi of 80, quiesced, and subjected to 15(S)-HETE-induced migration (A) or tube formation (B). C: C57BL/6 mice were injected subcutaneously with 0.5 ml of Matrigel premixed with vehicle or 50 μM 15(S)-HETE with and without Ad-GFP or Ad-dnATF-2 (5×10^9 pfu/ml). One week later, the animals were sacrificed, and the Matrigel plugs were harvested from underneath the skin and either immunostained for CD31 expression using anti-CD31 antibodies or analyzed for hemoglobin content using Drabkin's reagent. The values in the bar graphs in panels A, B, and C are the means ± SD of three independent experiments or four plugs from four animals. * $P < 0.01$ vs. Ad-GFP; ** $P < 0.01$ vs. Ad-GFP + 15(S)-HETE. The white bars represent controls to their respective treatments.

mutants inhibited 15(S)-HETE-induced MEK1 activation (**Fig. 8A, B**). Next we tested the role of MEK1 in 15(S)-HETE-induced JNK1 and ATF-2 activation. Blockade of MEK1 activation by adenovirus-mediated expression of its dominant negative mutant suppressed 15(S)-HETE-induced phosphorylation and activity of JNK1 and phosphorylation of ATF-2 (Fig. 8C, D). Recently, ω-6 PUFAs such as AA have been reported to stimulate proangiogenic processes, including enhancing the simultaneous effect of vascular endothelial growth factor (VEGF) and bFGF on angiopoietin-2 expression and tube formation in human endothelial cells (48). Because AA is the substrate for 15(S)-HETE production via the 15-LOX1/2 or 12-LOX pathways, we asked whether it has any effect on activation of ATF-2 in HRMVEC. As expected, AA (5 μM) stimulated the phosphorylation of ATF-2 in a time-dependent manner in HRMVEC (**Fig. 9A**). Similarly, AA (50 μM) induced Matrigel plug angiogenesis (Fig. 9B, C).

DISCUSSION

The important findings of the present study are that *1*) 15(S)-HETE activated Src, Rac1 and ATF-2 in a time-dependent manner in HRMVEC; *2*) 15(S)-HETE-induced ATF-2 activation was dependent on Src-Rac1-MEK1-JNK1

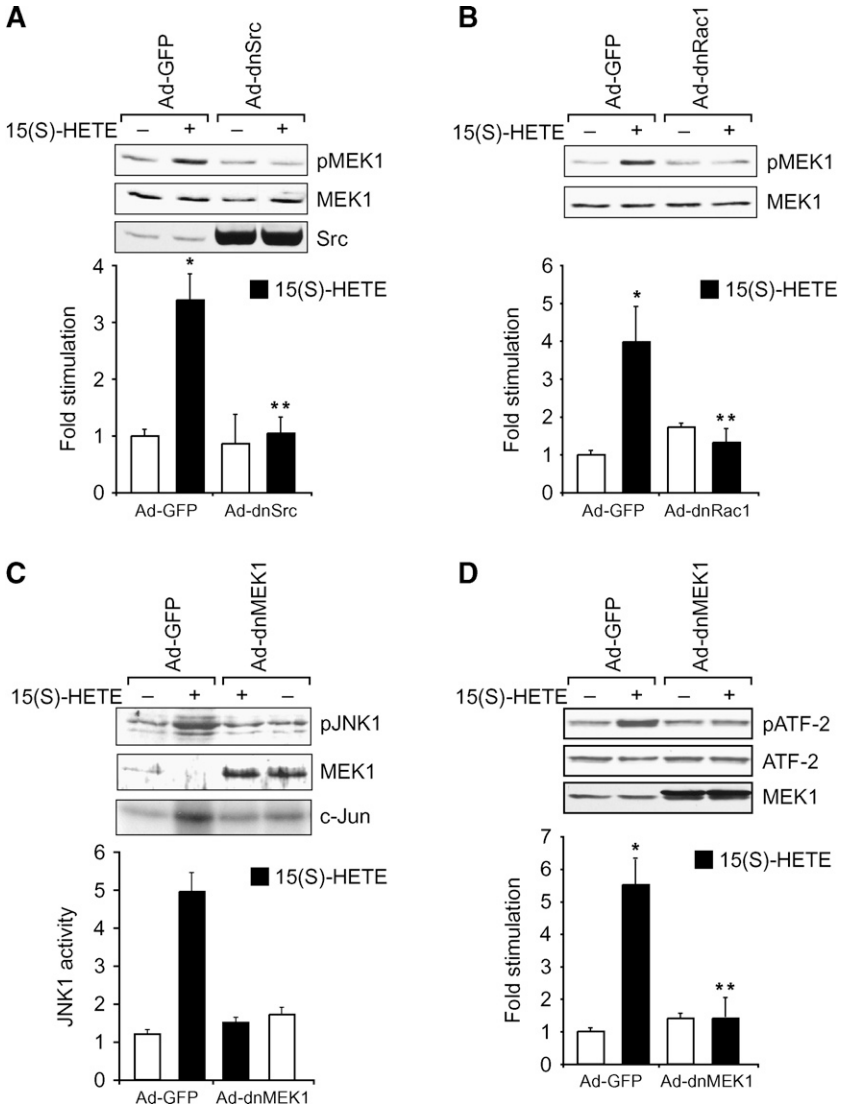

Fig. 8. Src-Rac1 signaling targets MEK1 in mediating JNK1-dependent ATF-2 activation in HRMVEC in response to 15(S)-HETE. A, B: HRMVEC were transduced with Ad-GFP, Ad-dnSrc, or Ad-dnRac1 at a moi of 80, quiesced, treated with and without 15(S)-HETE (0.1 μM) for 10 min, and cell extracts were prepared and analyzed for MEK1 activation by Western blotting using its phosphospecific antibodies. The blots were reprobed with anti-MEK1 antibodies for normalization. C, D: HRMVEC were transduced with Ad-GFP or Ad-dnMEK1 at a moi of 80, quiesced, treated with and without 15(S)-HETE (0.1 μM) for 10 min, and cell extracts were prepared and analyzed for JNK1 and ATF-2 phosphorylation using their phospho-specific antibodies. In panel C, an equal amount of protein from control and each treatment was also analyzed for JNK1 activity using immunocomplex kinase assay. In panel D, the blot was reprobed with anti-ATF-2 antibodies for normalization. The blots in panels A, B, C, and D were reprobed either with anti-MEK1 antibodies, anti-Src antibodies, or anti-ATF-2 antibodies for normalization or to show adenovirus-mediated overexpression of Src or MEK1. The values in the bar graphs in panels A, B, C, and D are the means ± SD of three independent experiments. * $P < 0.01$ vs. Ad-GFP; ** $P < 0.01$ vs. Ad-GFP + 15(S)-HETE. The white bars represent controls to their respective treatments.

signaling; and *3*) 15(S)-HETE-induced migration and tube formation of HRMVEC and Matrigel plug angiogenesis in vivo exhibited a requirement for activation of Src-Rac1-MEK1-JNK1-ATF-2 signaling. A large body of evidence indicates that Rac1 via its targeting of a wide variety of signaling molecules plays a role in the regulation of cell growth and in motility (30–32). One of the mechanisms of Rac1 activation by growth factors and cytokines is the involvement of tyrosine kinases such as the Src family of nonreceptor tyrosine kinases. A role for Src and Fyn in the activation of Rac1 by EGF and SCF in the mediation of intestinal epithelial cell and mast cell migration has been reported (43, 49). Similarly, the involvement of Src in the activation of Rac1 in mechanical strain-induced epithelial cell mitogenesis has been reported (50). Our results reveal that 15(S)-HETE, an eicosanoid, also possesses the capacity to activate Rac1 via

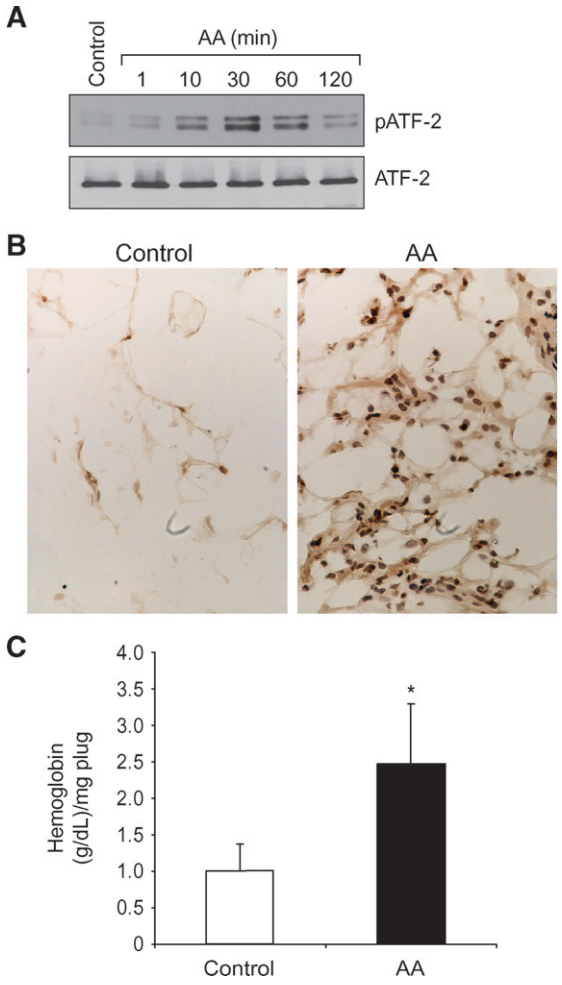

Fig. 9. AA stimulates phosphorylation of ATF-2 in HRMVEC in vitro and induces Matrigel plug angiogenesis in vivo. A: Quiescent HRMVEC were treated with and without AA (5 μM) for the indicated times, and cell extracts were prepared and analyzed by Western blotting for pATF-2 using its phosphospecific antibodies. B, C: C57BL/6 mice were injected subcutaneously with 0.5 ml of Matrigel premixed with vehicle or 50 μM AA. One week later, the animals were sacrificed, and the Matrigel plugs were harvested from underneath the skin and either immunostained for CD31 expression using anti-CD31 antibodies or analyzed for hemoglobin content using Drabkin's reagent. The values in the bar graph are the means ± SD of four plugs from four animals. * $P < 0.01$ vs. control.

recruiting Src as an upstream signaling molecule in the stimulation of HRMVEC migration and tube formation. It was reported that oxidants induce Src activation via the involvement of PKC (51). Many studies also showed that HETEs, including 15(S)-HETE, possess the capacity to activate PKC (52–54). Based on these findings, it is conceivable that 15(S)-HETE activates Src via a mechanism involving PKC. One study has reported that 12(S)-HETE binds to high affinity binding sites in the cytoplasm of lung carcinoma cells and thereby interacts with steroid receptor coactivator-1 (55). Although no further characterization was provided for these receptors, it is possible that 15(S)-HETE may also possess similar receptors in HRMVEC, which upon binding to 15(S)-HETE, may lead to activation of Src. While further studies are required for elucidation of the mechanisms by which 15(S)-HETE activates Src in HRMVEC, our results provide convincing evidence for the ability of 15(S)-HETE in the activation of this important nonreceptor tyrosine kinase leading to Rac1 activation in the mediation of migration and tube formation of these cells.

Rac1 plays a role in mediating receptor tyrosine kinase receptor and cytokine receptor-mediated signaling to activate JNK1 via recruiting MAPK kinase kinases, such as MEKK1-4, and MAPK kinases, such as MKK4/7 (56). Although, a role for MEKK1-4 and MKK4/7 cannot be ruled out in 15(S)-HETE-induced JNK1 activation, our previous observations revealed that PD98059, a potent inhibitor of MEK1/2 and a dominant negative mutant of MEK1 blocked 15(S)-HETE-induced JNK1 activation (8). In the present study, we showed that dnMEK1 also inhibits 15(S)-HETE-induced JNK1 activity. In addition, we found that suppression of Src-Rac1 signaling blocks 15(S)-HETE-induced MEK1 activation, suggesting that 15(S)-HETE activates JNK1 via Src-Rac1-MEK1-dependent mechanism in HRMVEC, leading to their migration and tube formation. A large body of data indicates that MEK1/2 phosphorylates and activates only ERK1/2 (56). However, our findings revealed a novel role for MEK1 in JNK1 activation as well, at least in human retinal microvascular endothelial cells. A role for MAPKs, particularly JNKs and p38MAPK, has been shown in the activation of ATF-2 (45–47). Similarly, a requirement for Rac1 activation in syndecan-4-induced ATF-2 transcriptional activity has been reported (57). Along with these findings, our observations show that 15(S)-HETE-induced ATF-2 activation depends on the Src-Rac1-MEK1-JNK1 signaling axis. In addition, because suppression of Src, Rac1, MEK1, and JNK1 inhibited ATF-2 activation and adenovirus-mediated expression of dominant negative ATF-2 mutant abrogated 15(S)-HETE-induced HRMVEC migration and tube formation, it appears that this transcriptional factor is an effector of Src-Rac1-MEK1-JNK1 activation signaling in the mediation of HRMVEC angiogenic differentiation by this eicosanoid.

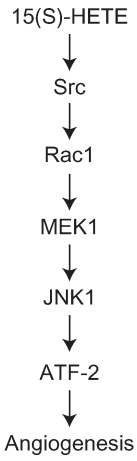

Fig. 10. Schematic diagram showing the potential mechanism of ATF-2 activation by 15(S)-HETE in the stimulation of HRMVEC angiogenic differentiation.

Furthermore, because adenovirus-mediated expression of dominant negative mutants of Src, Rac1, JNK1, MEK1, or ATF-2 negated 15(S)-HETE-induced Matrigel plug angiogenesis, it is likely that these signaling molecules may also influence angiogenesis in vivo in a manner similar to that seen in HRMVEC in vitro. Because AA, a substrate for the LOX enzymes, stimulated the phosphorylation of ATF-2 in HRMVEC in vitro and Matrigel plug angiogenesis in vivo, it is possible that similar signaling may also be effective in mediating angiogenesis by other hydroxy fatty acids such as 12(S)-HETE. Based on the efficacy of AA to induce Matrigel plug angiogenesis, it is possible to assume that besides its conversion via the cyclooxygenase, LOX, or cytochrome P450 monooxygenase (CYP) pathways, free fatty acid itself may induce angiogenesis.

Several studies have shown that hypoxia-induced angiogenesis requires FGF-2 and VEGF (58, 59). Previously, others and we have demonstrated that hypoxia induces the expression of 15-LOX1 and production of 15(S)-HETE in arteries and microvascular endothelial cells (8, 24, 60). In addition, we reported that 15(S)-HETE induces the expression of VEGF in human dermal microvascular endothelial cells (29). Based on these observations, it is possible that 15(S)-HETE may influence the expression of angiogenic factors such as FGF-2 and VEGF via activation of signaling pathways such as Src-Rac1-MEK1-JNK1-ATF-2 during hypoxia-induced angiogenesis. It was reported that lipoxin A_4, a metabolite of 15(S)-HETE, inhibits VEGF-induced angiogenesis (61). Based on this result, it may be conceivable that 15(S)-HETE-induced angiogenic differentiation of HRMVEC may not require its conversion to its metabolites.

In summary, the findings of the present study suggest that 15(S)-HETE-induced human retinal microvascular endothelial cell angiogenic differentiation requires Src-Rac1-MEK1-JNK1-dependent activation of ATF-2, as depicted in **Fig. 10.**

T.Z. performed cell migration and tube formation, immunocomplex kinase assays, pull-down assays, and Western blot analysis; D.W. performed Matrigel plug injections and immunohistochemistry; S.C. measured hemoglobin levels in Matrigel plugs; M.K. performed immunocomplex kinase assays and Western blot analysis; K.R.C. performed Western blot analysis; V.K.S. contributed in data analysis; D.A.J. provided collaborative discussions and participated in writing the manuscript; J.S.P. provided critical reagents and participated in collaborative discussions; G.N.R. designed the experiments, interpreted the data, and wrote the manuscript.

REFERENCES

1. Sigal, E., C. S. Craik, E. Highland, D. Grunberger, L. L. Costello, R. A. Dixon, and J. A. Nadel. 1988. Molecular cloning and primary structure of human 15-lipoxygenase. *Biochem. Biophys. Res. Commun.* **157:** 457–464.
2. Brash, A. R., W. E. Boeglin, and M. S. Chang. 1997. Discovery of a second 15(S)-lipoxygenase in humans. *Proc. Natl. Acad. Sci. USA.* **94:** 6148–6152.
3. Bryant, R. W., J. M. Bailey, T. Schewe, and S. M. Rapoport. 1982. Positional specificity of a reticulocyte lipoxygenase. Conversion of arachidonic acid to 15(S)-hydroperoxyeicosatetraenoic acid. *J. Biol. Chem.* **257:** 6050–6055.
4. Kilty, L., A. Logan, and P. J. Vickers. 1999. Differential characteristics of human 15-lipoxygenase isozymes and a novel splice variant of 15S-lipoxygenase. *Eur. J. Biochem.* **266:** 83–93.
5. Chang, M. S., C. Schneider, R. L. Roberts, S. B. Shappell, F. R. Haselton, W. E. Boeglin, and A. R. Brash. 2005. Detection and subcellular localization of two 15S-lipoxygenases in human cornea. Invest. *Ophthalmol. Vis. Sci.* **46:** 849–856.
6. Preston, I. R., N. S. Hill, R. R. Warburton, and B. L. Fanburg. 2006. Role of 12-lipoxygenase in hypoxia-induced rat pulmonary artery smooth muscle cell proliferation. *Am. J. Physiol.* **290:** L367–L374.
7. Reddy, M. A., Y. S. Kim, L. Lanting, and R. Natarajan. 2003. Reduced growth factor responses in vascular smooth muscle cells derived from 12/15-lipoxygenase-deficient mice. *Hypertension.* **41:** 1294–1300.
8. Bajpai, A. K., E. Blaskova, S. B. Pakala, T. Zhao, W. C. Glasgow, J. S. Penn, D. A. Johnson, and G. N. Rao. 2007. 15(S)-HETE production in human retinal microvascular endothelial cells by hypoxia: Novel role for MEK1 in 15(S)-HETE-induced angiogenesis. Invest. Ophthalmol. Vis. Sci. **48:**4930–4938.
9. Rao, G. N., A. S. Baas, W. C. Glasgow, T. E. Eling, M. S. Runge, and R. W. Alexander. 1994. Activation of mitogen-activated protein kinases by arachidonic acid and its metabolites in vascular smooth muscle cells. *J. Biol. Chem.* **269:** 32586–32591.
10. Yla-Herttuala, S., M. E. Rosenfeld, S. Parthasarthy, C. K. Glass, E. Sigal, J. L. Witztum, and D. Steinberg. 1990. Colocalization of 15-lioxygenase mRNA and protein with epitopes of oxidized low-density lipoprotein in macrophage-rich areas of atherosclerotic lesions. *Proc Natl Acad Sci USA.* **87:** 6959–6963.
11. Cyrus, T., J. L. Witztum, D. J. Rader, R. Tangirala, S. Fazio, M. F. Linton, and C. D. Funk. 1999. Disruption of the 12/15-Lipoxygenase gene diminishes atherosclerosis in apo E-deficient mice. *J. Clin. Invest.* **103:** 1597–1604.
12. Harats, D., A. Shaish, J. George, M. Mulkins, H. Kurihara, H. Levkovitz, and E. Sigal. 2000. Overexpression of 15-lipoxygenase in vascular endothelium accelerates early atherosclerosis in LDL receptor-deficient mice. *Arterioscler. Thromb. Vasc. Biol.* **20:** 2100–2105.
13. Henriksson, P., M. Hamberg, and U. Diczfalusy. 1985. Formation of 15-HETE as a major hydroxyeicosatetraenoic acid in the atherosclerotic vessel wall. *Biochim. Biophys. Acta.* **834:** 272–274.
14. Kelavkar, U. P., J. B. Nixon, C. Cohen, D. Dillehay, T. E. Eling, and K. F. Badr. 2001. Overexpression of 15-lipoxygenase-1 in PC-3 human prostate cancer cells increases tumorigenesis. *Carcinogenesis.* **22:** 1765–1773.
15. Shappel, S. B., S. J. Olson, S. E. Hannah, S. Manning, R. L. Roberts, N. Masumori, M. Jisaka, W. E. Boeglin, V. Vader, D. S. Dave, et al. 2003. Elevated expression of 12/15-lipoxygenase and cyclooxygenase-2 in a transgenic mouse model of prostate carcinoma. *Cancer Res.* **63:** 2256–2267.
16. Tang, S., B. Bhatia, C. J. Maldonado, P. Yang, R. A. Newman, J. Liu, D. Chandra, J. Traag, R. D. Klein, S. M. Fischer, et al. 2002. Evidence that arachidonate 15-lipoxygenase 2 is a negative cell cycle regulator in normal prostate epithelial cells. *J. Biol. Chem.* **277:** 16189–16201.
17. Bhatia, B., C. J. Maldonado, S. Tang, D. Chandra, R. D. Klein, D. Chopra, S. B. Shappell, P. Yang, R. A. Newman, and D. G. Tang. 2003. Subcellular localization and tumor-suppressive functions of 15-lipoxygenase 2 (15–LOX2) and its splice variants. *J. Biol. Chem.* **278:** 25091–25100.
18. Liu, B., R. J. Maher, J. P. DeJonckheere, R. U. Popat, S. Stojakovic, Y. A. Hannun, A. T. Porter, and K. V. Honn. 1997. 12(S)-HETE increases the motility of prostate tumor cells through selective activation of PKC alpha. *Adv. Exp. Med. Biol.* **400B:** 707–718.
19. Tang, D. G., C. Renaud, S. Stojakovic, C. A. Diglio, A. Porter, and K. V. Honn. 1995. 12(S)-HETE is a mitogenic factor for microvascular endothelial cells: its potential role in angiogenesis. *Biochem. Biophys. Res. Commun.* **211:** 462–468.
20. Shappel, S. B., R. A. Gupta, S. Manning, R. Whitehead, W. E. Boeglin, C. Schneider, T. Case, J. Price, G. S. Jack, T. M. Wheeler, et al. 2001. 15S-hydroxyeicosatetraenoic acid activates peroxisome proliferator-activated receptor gamma and inhibits proliferation in PC3 prostate carcinoma cells. *Cancer Res.* **61:** 497–503.
21. Shureiqi, I., D. Chen, R. Lotan, P. Yang, R. A. Newman, S. M. Fischer, and S. M. Lippman. 2000. 15-Lipoxygenase-1 mediates non-steroidal anti-inflammatory drug-induced apoptosis indepen-

dently of cyclooxygenase-2 in colon cancer cells. *Cancer Res.* **60:** 6846–6850.
22. Shureiqi, I., W. Jiang, X. Zuo, Y. Wu, J. B. Stimmel, L. M. Leesnitzer, J. S. Morris, H. Z. Fan, S. M. Fischer, and S. M. Lippman. 2003. The 15-lipoxygenase-1 product 13-S-hydroxyoctadecadienoic acid down-regulates PPAR-delta to induce apoptosis in colorectal cancer cells. *Proc. Natl. Acad. Sci. USA.* **100:** 9968–9973.
23. Graeber, J. E., B. M. Glaser, B. N. Setty, J. A. Jordan, R. W. Walenga, and M. J. Stuart. 1990. 15-Hydroxyeicosatetraenoic acid stimulates migration of human retinal microvessel endothelium in vitro and neovascularization in vivo. *Prostaglandins.* **39:** 665–673.
24. Setty, B. N., C. Ganley, and M. J. Stuart. 1985. Effect of changes in oxygen tension on vascular and platelet hydroxyacid metabolites. II. Hypoxia increases 15-hydroxyeicosatetraenoic acid, a proangiogenic metabolite. *Pediatrics.* **75:** 911–915.
25. Folkman, J. 1995. Angiogenesis in cancer, vascular, rheumatoid and other disease. *Nat. Med.* **1:** 27–31.
26. Khurana, R., M. Simons, J. F. Martin, and I. C. Zachary. 2005. Role of angiogenesis in cardiovascular disease: a critical appraisal. *Circulation.* **112:** 1813–1824.
27. Gariano, R. F., and T. W. Gardner. 2005. Retinal angiogenesis in development and disease. *Nature.* **438:** 960–966.
28. Zhang, B., H. Cao, and G. N. Rao. 2005. 15(S)-Hydroxyeicosatetraenoic acid induces angiogenesis via activation of PI3K-Akt-mTOR-S6K1 signaling. *Cancer Res.* **65:** 7283–7291.
29. Srivastava, K., V. Kundumani-Sridharan, B. Zhang, A. K. Bajpai, and G. N. Rao. 2007. 15(S)-Hydroxyeicosatetraenoic acid-induced angiogenesis requires signal transducer and activator of transcription-3-dependent expression of vascular endothelial growth factor. *Cancer Res.* **67:** 4328–4336.
30. Raftopoulou, M., and A. Hall. 2004. Cell migration: Rho GTPases lead the way. *Dev. Biol.* **265:** 23–32.
31. Liu, W. F., C. M. Nelson, D. M. Pirone, and C. S. Chen. 2006. E-cadherin engagement stimulates proliferation via Rac1. *J. Cell Biol.* **173:** 431–441.
32. Guo, F., M. Debidda, L. Yang, D. A. Williams, and Y. Zheng. 2006. Genetic deletion of Rac1 GTPase reveals its critical role in actin stress fiber formation and focal adhesion complex assembly. *J. Biol. Chem.* **281:** 18652–18659.
33. Teramoto, H., O. A. Coso, H. Miyata, T. Igishi, T. Miki, and J. S. Gutkind. 1996. Signaling from the small GTP-binding proteins Rac1 and Cdc42 to the c-Jun N-terminal kinase/stress activated protein kinase pathway. A role for mixed lineage kinase 3/protein-tyrosine kinase 1, a novel member of the mixed lineage kinase family. *J. Biol. Chem.* **271:** 27225–27228.
34. Liu, Z., C. Zhang, N. Dronadula, Q. Li, and G. N. Rao. 2005. Blockade of nuclear factor of activated T cells activation signaling suppresses balloon injury-induced neointima formation in a rat carotid artery model. *J. Biol. Chem.* **280:** 14700–14708.
35. Coso, O. A., M. Chiariello, J. C. Yu, H. Teramoto, P. Crespo, N. Xu, T. Miki, and J. S. Gutkind. 1995. The small GTP-binding proteins Rac1 and Cdc42 regulate the activity of the JNK/SAPK signaling pathway. *Cell.* **81:** 1137–1146.
36. Derijard, B., M. Hibi, I. H. Wu, T. Barrett, B. Su, T. Deng, M. Karin, and R. J. Davis. 1994. JNK1: a protein kinase stimulated by UV light and Ha-Ras that binds and phosphorylates the c-Jun activation domain. *Cell.* **76:** 1025–1037.
37. Beier, F., R. J. Lee, A. C. Taylor, and R. G. Pestell. 1999. LuValle P. Identification of the cyclin D1 gene as a target of activating transcription factor 2 in chondrocytes. *Proc. Natl. Acad. Sci. USA.* **96:** 1433–1438.
38. Berkner, K. L. 1988. Development of adenovirus vectors for the expression of heterologous genes. *Biotechniques.* **6:** 616–629.
39. Fulton, D., J. E. Church, L. Ruan, C. Li, S. G. Sood, B. E. Kemp, I. G. Jennings, and R. C. Venema. 2005. Src kinase activates endothelial nitric oxide synthase by phosphorylating Tyr-83. *J. Biol. Chem.* **280:** 35943–35952.
40. Madamanchi, N. R., R. D. Bukoski, M. S. Runge, and G. N. Rao. 1998. Arachidonic acid activates jun N-terminal kinase in vascular smooth muscle cells. *Oncogene.* **16:** 417–422.
41. Nagata, D., M. Mogi, and K. Walsh. 2003. AMP-activated protein kinase (AMPK) signaling in endothelial cells is essential for angiogenesis in response to hypoxic stress. *J. Biol. Chem.* **278:** 31000–31006.
42. Medhora, M., J. Daniels, K. Mundey, B. Fisslthaler, R. Busse, E. R. Jacobs, and D. R. Harder. 2003. Epoxygenase-driven angiogenesis in human lung microvascular endothelial cells. *Am. J. Physiol.* **284:** H215–H224.
43. Dise, R. S., M. R. Frey, R. H. Whitehead, and D. B. Polk. 2008. Epidermal growth factor stimulates Rac activation through src and phosphatidylinositol 3-kinase to promote colonic epithelial cell migration. *Am. J. Physiol.* **294:** G276–G285.
44. DerMardirossian, C., G. Rocklin, J. Y. Seo, and G. M. Bokoch. 2006. Phosphorylation of RhoGDI by Src regulates Rho GTPase binding and cytosol-membrane cycling. *Mol. Biol. Cell.* **17:** 4760–4768.
45. Gupta, S., D. Campbell, B. Derijard, and R. J. Davis. 1995. Transcription factor ATF-2 regulation by the JNK signal transduction pathway. *Science.* **267:** 389–393.
46. Van Dam, H., D. Wilhelm, I. Herr, A. Steffen, P. Herrlich, and P. Angel. 1995. ATF-2 is preferentially activated by stress-activated protein kinases to mediate c-jun induction in response to genotoxic agents. *EMBO J.* **14:** 1798–1811.
47. Sano, Y., H. Akimaru, T. Okamura, T. Nagao, M. Okada, and S. Ishii. 2005. Drosophila activating transcription factor-2 is involved in stress response via activation by p38, but not c-Jun NH(2)-terminal kinase. *Mol. Biol. Cell.* **16:** 2934–2946.
48. Szymczak, M., M. Murray, and N. Petrovic. 2008. Modulation of angiogenesis by ω-3 polyunsaturated fatty acids is mediated by cyclooxygenases. *Blood.* **111:** 3514–3521.
49. Samayawardhena, L. A., R. Kapur, and A. W. Craig. 2007. Involvement of Fyn kinase in Kit and integrin-mediated Rac activation, cytoskeletal reorganization, and chemotaxis of mast cells. *Blood.* **109:** 3679–3686.
50. Chaturvedi, L. S., H. M. Marsh, X. Shang, Y. Zheng, and M. D. Basson. 2007. Repetitive deformation activates focal adhesion kinase and ERK mitogenic signals in human Caco-2 intestinal epithelial cells through Src and Rac1. *J. Biol. Chem.* **282:** 14–28.
51. Rosado, J. A., P. C. Redondo, G. M. Salido, E. Gomez-Arteta, S. O. Sage, and J. A. Pariente. 2004. Hydrogen peroxide generation induces pp60Src activation in human platelets:evidence for the involvement of this pathway in store-mediated calcium entry. *J. Biol. Chem.* **279:** 1665–1675.
52. Szekeres, C. K., K. Tang, M. Trikha, and K. V. Honn. 2000. Eicosanoid activation of extracellular signal-regulated kinase 1/2 in human epidermoid carcinoma cells. *J. Biol. Chem.* **275:** 38831–38841.
53. Sharma, G. D., P. Ottino, N. G. Bazan, and H. E. Bazan. 2005. Epidermal and hepatocyte growth factors, but not keratinocyte growth factor, modulate protein kinase Calpha translocation to the plasma membrane through 15(S)-hydroxyeicosatetraenoic acid synthesis. *J. Biol. Chem.* **280:** 7917–7924.
54. Mikule, K., S. Sunpaweravong, J. C. Gatlin, and K. H. Pfenninger. 2003. Eicosanoid activation of protein kinase epsilon:involvement in growth cone repellent signaling. *J. Biol. Chem.* **278:** 21168–21177.
55. Kurahashi, Y., H. Herbertsson, M. Soderstrom, M. G. Rosenfeld, and S. Hammarstrom. 2000. A 12(S)-hydroxyeicosatetraenoic acid receptor interacts with steroid receptor coactivator-1. *Proc. Natl. Acad. Sci. USA.* **97:** 5779–5783.
56. Davis, R. J. 2000. Signal transduction by the JNK group of MAP kinases. *Cell.* **103:** 239–252.
57. Saoncella, S., E. Calautti, W. Neveu, and P. F. Goetinck. 2004. Syndecan-4 regulates ATF-2 transcriptional activity in a Rac1-dependent manner. *J. Biol. Chem.* **279:** 47172–47176.
58. Calvani, M., A. Rapisarda, B. Uranchimeg, R. H. Shoemaker, and G. Melillo. 2006. Hypoxic induction of an HIF-1alpha-dependent bFGF autocrine loop drives angiogenesis in human endothelial cells. *Blood.* **107:** 2705–2712.
59. Shweiki, D., A. Itin, D. Soffer, and E. Keshet. 1992. Vascular endothelial growth factor induced by hypoxia may mediate hypoxia-initiated angiogenesis. *Nature.* **359:** 843–845.
60. Zhu, D., M. Medhora, W. B. Campbell, N. Spitzbarth, J. E. Baker, and E. R. Jacobs. 2003. Chronic hypoxia activates lung 15-lipoxygenase, which calalyzes production of 15-HETE and enhances constriction in neonatal rabbit pulmonary arteries. *Circ. Res.* **92:** 992–1000.
61. Fierro, I. M., J. L. Kutok, and C. N. Serhan. 2002. Novel lipid mediator regulators of endothelial cell proliferation and migration: aspirin-triggered-15R-lipoxin A_4 and lipoxin A_4. *J. Pharmacol. Exp. Ther.* **300:** 385–392.